OXFORD

Food Quality and Safety, 2021, 5, 1–11
doi:10.1093/fqsafe/fyaa032
Article

Article

Assessment of chicken breast shelf life based on bench-top and portable near-infrared spectroscopy tools coupled with chemometrics

Ilaria Lanza[1], Daniele Conficoni[1], Stefania Balzan[2], Marco Cullere[1], Luca Fasolato[2], Lorenzo Serva[1], Barbara Contiero[1], Angela Trocino[2], Giorgio Marchesini[1], Gerolamo Xiccato[3], Enrico Novelli[2] and Severino Segato[1]

[1]Department of Animal Medicine, Productions and Health, University of Padova, Legnaro, Italy; [2]Department of Comparative Biomedicine and Food Science, University of Padova, Legnaro, Italy and [3]Department of Agronomy, Food, Natural Resources, Animals and Environment, University of Padova, Legnaro, Italy

Correspondence to: Luca Fasolato, Department of Comparative Biomedicine and Food Science, University of Padova, 35020 Legnaro (PD), Italy. E-mail: luca.fasolato@unipd.it

Received 7 September 2020; Revised 12 November 2020; Editorial decision 15 November 2020.

Abstract

Objectives: Near-infrared (NIR) spectroscopy is a rapid technique able to assess meat quality even if its capability to determine the shelf life of chicken fresh cuts is still debated, especially for portable devices. The aim of the study was to compare bench-top and portable NIR instruments in discriminating between four chicken breast refrigeration times (RT), coupled with multivariate classifier models.

Materials and Methods: Ninety-six samples were analysed by both NIR tools at 2, 6, 10 and 14 days post mortem. NIR data were subsequently submitted to partial least squares discriminant analysis (PLS-DA) and canonical discriminant analysis (CDA). The latter was preceded by double feature selection based on Boruta and Stepwise procedures.

Results: PLS-DA sorted moderate separation of RT theses, while shelf life assessment was more accurate on application of Stepwise-CDA. Bench-top tool had better performance than portable one, probably because it captured more informative spectral data as shown by the variable importance in projection (VIP) and restricted pool of Stepwise-CDA predictive scores (SPS).

Conclusions: NIR tools coupled with a multivariate model provide deep insight into the physicochemical processes occurring during storage. Spectroscopy showed reliable effectiveness to recognise a 7-day shelf life threshold of breasts, suitable for routine at-line application for screening of meat quality.

Graphical Abstract

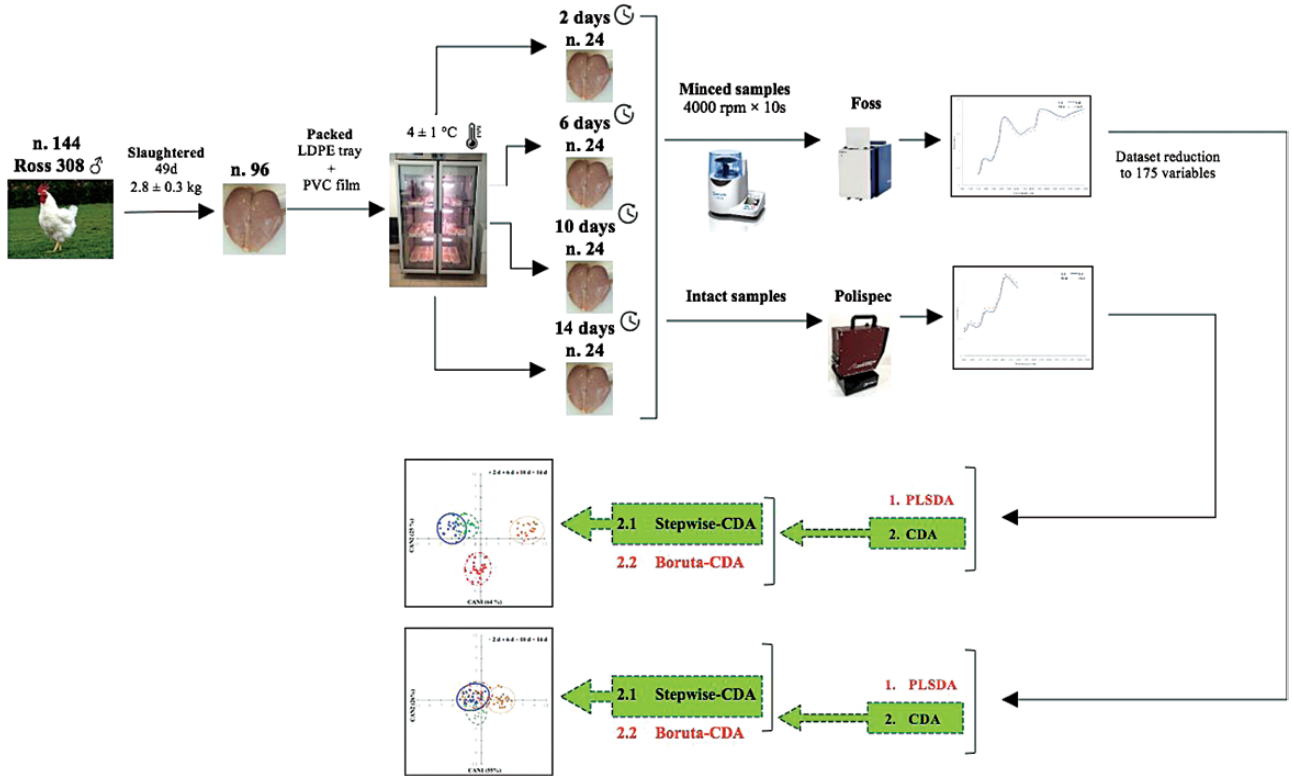

Key words: shelf life; chicken breast; Near-infrared (NIR) spectroscopy; bench-top NIR; portable NIR; canonical discriminant analysis.

Introduction

Globally, about 127 million tonnes of poultry meat is produced per year, making it the biggest meat sector worldwide (FAO, 2020a). The low price, valuable nutritional profile, mild sensory attributes, ease of cooking and cultural acceptability are all key factors pushing the market development of chicken meat (FAO, 2020b; Katiyo *et al.*, 2020). As for meat in general, the high nutrient and moisture content as well as the tendentially higher pH of fresh chicken meat make it highly perishable, leading to a fast loss of freshness during storage (Fernández-Pan *et al.*, 2014; Katiyo *et al.*, 2020). Inappropriate storage conditions (e.g. temperature variations, inadequate packaging and prolonged shelf life) can result in product discoloration, accumulation of off-flavours and off-odours, and alteration of sensory traits, ultimately making meat consumption unsuitable (Sivarajan *et al.*, 2017). Given poultry meat's relatively short shelf life (Fernández-Pan *et al.*, 2014), preservation of quality during refrigerated storage represents one of the main challenges for the poultry industry. Currently, meat ageing can be assessed by sensory, enzymatic, DNA-based, microbiological, bio-imaging and spectroscopic analytical approaches. However, non-spectroscopic methods are laborious, time-consuming and destructive and also require sophisticated laboratory procedures (Alamprese *et al.*, 2016; Falkovskaya *et al.*, 2019). Due to the dynamism of the meat industry, a cost-effective and non-destructive quality control system to assess meat freshness is therefore needed (Teixeira dos Santos *et al.*, 2013; Mendez *et al.*, 2019).

In this context, near-infrared (NIR) spectroscopy is a fast, eco-friendly, non-invasive and reliable technology for the analysis and authentication of a wide range of meat products (Morsy and Sun, 2013; Mendez *et al.*, 2019), for predicting chicken cut differentiation (Nolasco Perez *et al.*, 2018), identifying breed origin (Ding *et al.*, 1999), quality attributes (Barbin *et al.*, 2015) and spoilage (Alexandrakis *et al.*, 2012), and for the discrimination of fresh from frozen–thawed poultry meat (Atanassova *et al.*, 2018). NIR radiation ranges from 780 to 2500 nm on the electromagnetic spectrum. The interaction of this radiation with meat samples results in weak and broad absorption bands that must be analysed through multivariate analysis methods, coupled with spectral pre-processing techniques for clear data interpretation (Teixeira dos Santos *et al.*, 2013; Zareef *et al.*, 2020). Recently, considerable attention has been given to portable spectroscopic devices due to their valuable advantages compared to stationary ones. Portable spectrometers are lightweight and easy-to-use tools that allow direct, non-destructive and *in situ* sample measurement. Furthermore, they avoid laboratory transportation (time and cost saving), improve the efficiency of the testing process and provide the knowledge to make informed decisions on the spot (Teixeira dos Santos *et al.*, 2013; Crocombe, 2018).

Based on the above-mentioned premises, our aim was to evaluate the feasibility of using bench-top and portable NIR spectroscopy instruments for discriminating chicken breasts during a 14-day refrigeration period. The reliability of the portable NIR tool for a real time control of meat shelf life to make on-the-spot evaluations

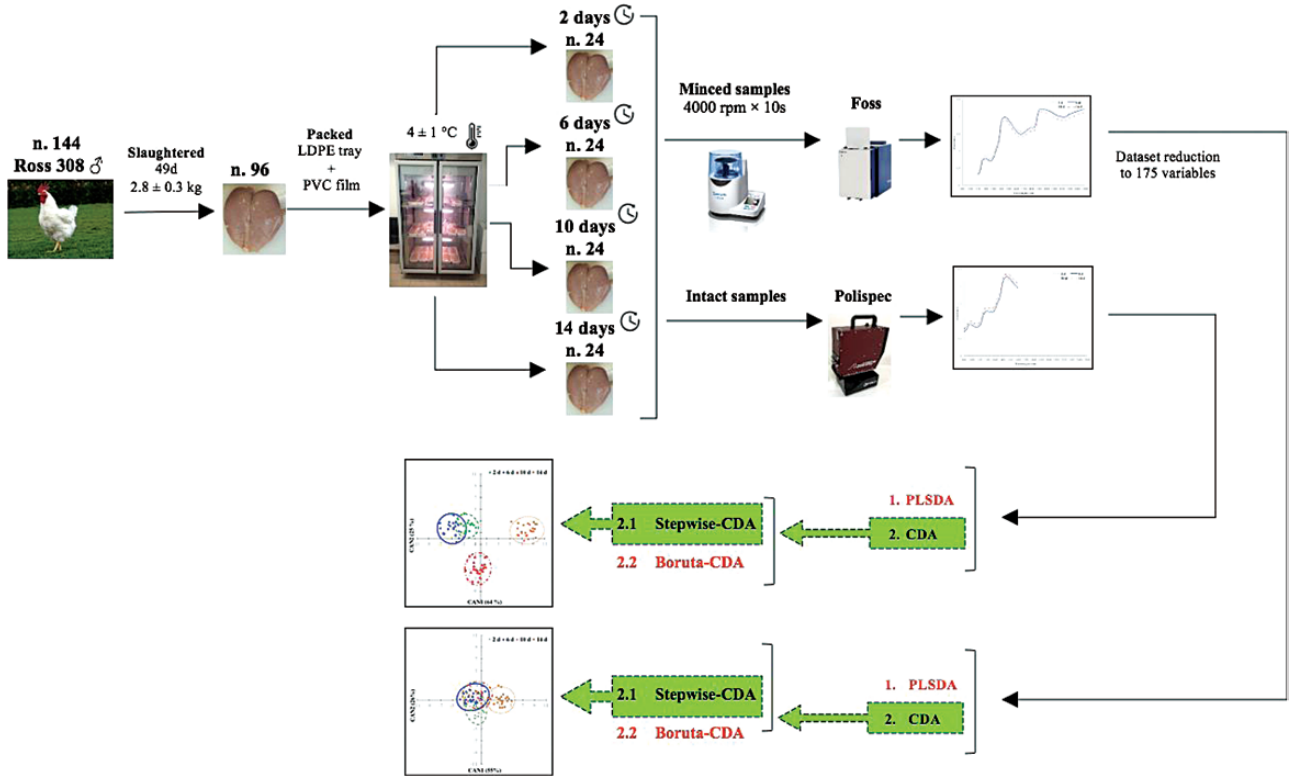

Figure 1. Flow chart of the experimental design: sampling, setting refrigeration time theses, acquiring NIR spectra and predicting discriminative modelling. LDPE, low-density polyethylene; PLSDA, partial least square-discriminant analysis; CDA, canonical discriminant analysis; NIR, near-infrared.

along supply chain, was compared to the well-known predictive performance of the bench-top instrument. An in-depth description of the interaction among electromagnetic radiation and alteration pathways aiming at obtaining detailed information about the physicochemical changes occurring during poultry meat shelf life. This comparative analysis of the spectroscopy behaviour was related to a restricted pool of informative NIR wavelengths selected by two multivariate discriminative models.

Materials and Methods

Experimental design and meat sampling

The study was conducted under ethical approval (project 17/2016; No 154392 of the 10 May 2016) of the Ethical Committee for Animal Experimentation of the University of Padova to perform experiments on animals. Moreover, all efforts were made to curtail the animal suffering throughout the trial.

A total of 96 male Ross 308 chickens were slaughtered (carcass weight: 2.8 ± 0.3 kg) in a commercial plant at 49 days old. After stunning, exsanguination, plucking and evisceration of birds, breast muscles were dissected (0.88 ± 0.09 kg as averaged weight), immediately (first experimental day) packed in low-density polyethylene trays wrapped in a 12 µm-thick PVC film (Weegal, KOEX 412, Gruppo Fabbri, Vignola, Modena, Italy) and stored in a refrigerated cabinet (Majolo® Plus 100 Seasoning Controller, Majolo, Cadoneghe, Padova, Italy). The storage was designed to simulate commercial refrigeration setting conditions: samples were exposed to a 36 W fluorescent lamp light for about 12 h daily (from 8 a.m. to 8 p.m.), and then in dark during night (from 8 p.m. to 8 a.m.), always keeping a temperature of 4 ± 1 °C.

As reported in Figure 1, to assess meat freshness during the shelf life by NIR spectroscopy, breasts were randomly grouped into four theses (n = 24) corresponding to the following refrigeration times (RT), as days *post mortem*: ≤2 (2 d), 3–6 (6 d), 7–10 (10 d) and 11–14 (14 d).

Chemical and sensorial analyses on breast samples

The breast samples were analyzed according to the set storage time (after 2, 6, 10 and 14 days post mortem) to measure their physicochemical and sensorial traits. The pH was recorded in triplicate with a portable pH-meter (KnickPortamess® 911, Berlin, Germany) equipped with a penetrating electrode (5 mm diameter conic tip, Crison 5232, Modena, Italy). Colour (averaged of 5 areas on the breast surface) was measured by a Konica Minolta CD-600 visible spectrophotometer (Konica Minolta Sensing, Inc., Osaka, Japan), applying CIE L*a*b* system (L*, lightness; a*, redness; b*, yellowness) with D65 as light source and 10° observed angle (Melro *et al.*, 2020). Drip loss was determined by weighing of 2.5 cm-slice cut from the surface of dorsal breast, which was packaged in polyethylene bags and kept overnight at 2 ± 1 °C. Drip loss (%) was calculated by the following equation: [(initial weight – final weight)/initial weight]. Sensory evaluation was conducted by a panel consisting of 10 trained students and researchers of the School of Agricultural Sciences and Veterinary Medicine of Padova University, and sensory traits (odour, texture and colour) were scored according to Raab *et al.* (2008) using a demerit 3-point scoring system (1 = not acceptable, 2 = acceptable, 3 = good quality). A synthetic sensory index (SI) was calculated as: [(2 × odour score + 2 × colour score + 1 × texture score)/5], with 1.8 score as the threshold to define spoiled samples (Raab *et al.*, 2008).

NIR spectroscopy analysis

As reported in Figure 1, after 2, 6, 10 and 14 days post mortem, chicken breast samples were analysed (at 18 ± 2 °C) within 45 ± 10 min using both a bench-top FOSS NIRSystems 5000 analyser (FOSS Analytical A/S, Hillerød, Denmark) and a portable Polispec NIR (PoliSPEC^{NIR}, ITPhotonics, Breganze, Italy).

For the lab-scale system (referred to as Foss) a right-side breast subsample (around 125 g) was minced at 4000 rpm for 10 s with a Grindomix GM200 knife mill (Retsch GmbH, Haan, Germany) and then poured and gently compressed into a small ring cup with a quartz window that allowed irradiation of an area of about 9.6 cm^2. Spectral data were recorded in duplicate by covering a range of 1100–2500 nm at 2 nm intervals. The instrument was equipped with a spinning module, and spectra were collected in reflectance mode, averaging 32 scans of the sample after 16 internal references.

For the portable system (referred to as Polispec), the raw left side of the breast (not minced) was submitted to NIR analysis through an embedded 3.2 cm^2 quartz cylinder probe for 10 s scanning time, thus covering around a 10 cm^2 meat surface; spectra were acquired in reflectance mode (900–1600 nm at 2 nm intervals), in duplicate. Each scan lasted 5 s (about 10 ms of integration time), covering about 10 cm^2 of the sample area.

For both NIR instruments, spectral data were recorded as absorbance (A) calculated as log(1/R), where R is the reflectance of the sample, by using WinISI 2 software V1.05 (Infrasoft International Inc., Port. Matilda, USA) and poliDATA (ITPhotonics, Breganze, Italy), for bench-top and portable instrument, respectively. Spectra were subsequently exported in .csv format for further chemometric analysis. Prior to statistical analysis, spectra of the two replicates were averaged. For both instruments, in order to reduce light scattering and to remove the baseline shift, smoothing, standard normal variate (SNV), first-order derivative and detrend transformations were applied (Bisutti *et al.*, 2019).

Statistical and chemometric analyses

Regarding meat quality variables, the assumption of normality was tested using the Shapiro-Wilk test (PROC UNIVARIATE). Then, instrumental colour, pH and drip loss data were submitted to a one-way ANOVA (PROC GLM) to test the effect of RT. The hypotheses of the linear model (normality, independence and homoscedasticity) were visually assessed on the residuals. Post hoc pairwise multiple comparisons among levels were conducted using Bonferroni correction. Orthogonal contrasts were performed to assess the linear and quadratic components of RT effect. Data not normally distributed (sensory traits) were analysed using a non-parametric Kruskal–Wallis test. Post-hoc multiple pairwise comparisons were conducted using the Steel–Dwass–Critchlow–Fligner procedure (based on the averaged ranks). The SAS software (release 9.4, SAS Institute Inc., Cary, USA) was used for all the above-mentioned analyses.

Then, partial least square-discriminant analysis (PLS-DA) and canonical discriminant analysis (CDA) statistical modelling approaches were applied on the NIR spectral variables of both spectrometers to discriminate among the 2 d, 6 d, 10 d and 14 d RT theses. The PLS-DA multivariate classifier model was performed using the PLS Toolbox (PLS Toolbox, V5.8.2.1, Eigenvector Research, Inc., Manson, WA, USA) of MATLAB software (v 9.2.0 538062; The MathWorks Inc., Natick, MA, USA). Smoothing, SNV, first-order derivative and detrend transformations gave better results for bench-top, while no pre-treatments were carried out for portable system. The reliability of PLS-DA was assessed by a cross-validation performing a venetian blind algorithm with 10 splits and one sample per split (Rubingh *et al.*, 2006). Furthermore, variable importance in projection (VIP), used to highlight the most influential absorbance wavelengths, was calculated using the relevance of predictors according to the PLS-DA threshold criterion of 'greater than one' (Ottavian *et al.*, 2015).

Despite CDA is reported as multivariate model able to improve the classification performance by using a high number of closed-spectral variables, a discriminative process based on a dataset of many highly correlated variables could not retain some informative wavelengths. Therefore, prior to application of supervised CDA, the bench-top dataset was arranged reducing averaged spectral variables to 175 (Akarachantachote *et al.*, 2014), each referring to an 8 nm interval range, so that the mean value was assigned by interpolating the R values to the intermediate wavelength (from λ_{1106}, equal to the average of R from 1102 to 1110 nm, to λ_{2490}, equal to the average of R from 2486 to 2494 nm). Double feature selection was carried out as the preliminary step of the CDA. The first (named Boruta) was based on the Boruta random forest feature selection (Kursa and Rudnicki, 2010), using an R software package (Comprehensive R Archive Network, R Development Core Team, 2010). The second (named Stepwise) was run within the forward Stepwise procedure (PROC STEPWISE) of SAS software. Both Boruta and Stepwise features were submitted to the last step of CDA (PROC CANDISC of SAS) to achieve the most discriminative analysis by maximising the distance among RT theses, and their degree of dissimilarity was measured by squared Mahalanobis distances (D^2-Mahalanobis). The outcomes of the CDA were plotted according to the main canonical functions CAN1 and CAN2 using XLSTAT software (release 2016, Addinsoft, New York, USA). The reliability of the CDA was assessed by a confusion matrix obtained by a cross-validation based on the leave-one-out criterion (PROC DISCRIM of SAS).

The metrics depicted in the confusion matrices used to assess the goodness of the classification performance of the PLS-DA and CDA models were the following descriptive statistics (Segato *et al.*, 2019): accuracy, sensitivity, specificity, precision and Matthews correlation coefficient (MCC).

Results and Discussion

Assurance of meat quality related to shelf life assessment has led to the design of models based on rapid and non-destructive high-throughput techniques. In this study, three targeted multivariate classifier models, PLS-DA, Boruta-CDA (random forest selection) and Stepwise-CDA (targeted selection), were built using the NIR spectral data from bench-top and portable NIR spectrometers. Their efficiency to predict chicken breast shelf life was evaluated according to four classes of freshness (days *post-mortem*): fresh (2 d), acceptable (6 d), spoiled (10 d) and rotten (14 d). Fresh and acceptable theses guarantee safety and maintain the overall quality attributes with respect to consumer preferences. During storage, shifts in biochemical pathways and spoiling microbial populations occur, leading to changes in meat appearance. Detrimental sensorial decay usually starts after a chilled storage period that coincides with a cut-off between the end of the acceptable and the beginning of the spoiled thesis. Since poultry meat is a highly perishable food, the predominant organisms and biochemical changes lead to intense proteolysis, amino acid degradation and lipid oxidation that at the end of storage (rotten thesis with more of 10 days of refrigerated storage) induce

the formation of by-products associated with the production of off-flavour and slime, thus prejudicing consumer acceptability (Gram *et al.*, 2002; Bruckner *et al.*, 2012).

Chemical and sensorial analyses

As reported in Table 1, RT significantly affected the physicochemical and sensorial traits of chicken breast samples. The pH values showed a linear increase ($P < 0.001$) after six days of refrigeration mainly due to the proliferation of spoilage microorganisms as reported by Sujiwo *et al.* (2018). Meat colour showed a significant change of L*: in detail, an initial decrease in lightness was observed after six days followed by a progressive increase in the latest conservation time (*P*-value of the quadratic component of variance < 0.001). This trend was related to changes in water retention ability and myofibrils structure along the storage period which affected the content of free water in meat. Moreover, during storage, a significant increase of drip losses was recorded which increased the lightness because water previously bound to myofibrils was released (Gratta *et al.*, 2019). The sensorial traits (odour, colour and texture) were associated to the highest level of freshness until six days of conservation, after which the SI (meat acceptability) decreased (Table 1). A detrimental effect of RT was observed for the rotten samples (thesis 14 d) that showed the lowest values of odour and colour contributing to an unacceptable (<1.8) SI (Raab *et al.*, 2008). The results of the sensorial evaluation defined a cut-off between 6 (fresh meat) and 10 (spoiled meat) days since at least 25% of 10 d-poultry breast samples had a SI value lower than 1.8 (Figure 2). The metabolism of spoilage bacteria leading to the formation of by-products associated with off-flavour and slime production, prejudicing acceptability in the rotten samples.

Shelf life assessment by PLS-DA

As reported in Table 2, the performance of the PLS-DA model in predicting the four chicken breast RT theses was moderately accurate, highlighting an overall better discriminative capacity for the bench-top instrument (MCC > 0.75) compared to portable (MCC > 0.35) one. The higher accuracy (>0.91) and precision (>0.83) values for the bench-top instrument are probably linked to the meat mincing pre-process. Muscle grinding tends to improve discriminative performance, reducing sample heterogeneity (i.e. texture, colour and proximate composition) and increasing the repeatability of NIR spectrum acquisition (Xu *et al.*, 2019). Moreover, analysis of intact muscles is susceptible to the effect of the high moisture content on the surface as well as fine subcutaneous fat, even if samples are well trimmed. The lower discriminative capability of the portable tool might be also explained by the size of the measuring head, the distinctive optical properties and the detector type, which must be resized in order to miniaturise the NIR device, resulting in a shorter spectral wavelength range (Teixeira dos Santos *et al.*, 2013).

Shelf life assessment by CDA

The main purpose of the research was to evaluate the feasibility of using NIR spectroscopy to predict chicken breast shelf life: for this purpose, further multivariate modelling was performed. CDA seemed to improve the spatial separation of the experimental groups, but could not work efficiently in the case of a large dataset with too many irrelevant and highly correlated variables obscuring the informative ones and worsening the discriminative performance (Leardi, 2000; Zhao and Maclean, 2000). Since the CDA algorithm allows a reduction of redundancy (Akarachantachote *et al.*, 2014), before the Stepwise selection, a spectral arrangement was carried out on the bench-top dataset, restricting it to 175 averaged spectral variables so that each one represented an 8 nm wavelength range (from λ_{1106} to λ_{2490}). Since the portable system was characterised by a shorter spectral acquisition time, there was no need to restrict the original dataset.

As described above, four CDAs were performed using two preliminary feature selections (Stepwise vs Boruta) for each instrument (bench-top vs portable). A summary of the predictive performance of this CDA set is reported in Table 3. Both NIR instruments had a lower value of Wilks' λ, a test statistic that is minimised within the procedure in order to obtain the widest spatial segregation of the experimental groups, when the algorithm was performed with the preliminary Stepwise criterion as feature selection. The better discriminative capacity of the preliminary Stepwise procedure was also assessed by higher D^2-Mahalanobis values than those observed for Boruta (Table 3).

Thus, we focus the discussion on the Stepwise forward CDA being the most accurate fitting model.

For the lab-scale NIR tool, the Stepwise procedure selected 32 significant averaged wavelengths (Table 3). These spectral variables were used to perform the CDA algorithm that defined two

Table 1. Effect of the refrigeration time (RT) on pH, colour (CIE L*a*b*), drip losses and sensorial attributes of chicken breasts

Quality traits	Refrigeration time (RT)				SEM	*P*-value		
	2 d	6 d	10 d	14 d		Global	Linear	Quadratic
pH	5.92^{c}	5.96^{c}	6.12^{b}	6.18^{a}	0.02	<0.001	<0.001	0.034
L* (lightness)	47.0^{ab}	45.7^{b}	45.7^{b}	48.1^{a}	0.6	0.014	0.249	0.003
a* (redness)	1.8^{ab}	2.2^{a}	1.8^{ab}	1.8^{b}	0.1	0.029	0.316	0.067
b* (yellowness)	10.6^{ab}	11.3^{a}	10.1^{b}	10.1^{b}	0.3	0.034	0.096	0.308
Drip losses (%)	3.0^{b}	3.8^{a}	3.4^{ab}	n. e.[1]	0.2	0.006	0.096	0.006
Sensorial analysis[2]								
Odour	3.0 (3.0-3.0)^{a}	3.0 (3.0-3.0)^{a}	2.5 (1.0–3.0)^{b}	1.0 (1.0–2.0)^{c}		<0.001		
Colour	3.0 (2.0–3.0)^{a}	3.0 (2.0–3.0)^{a}	2.0 (1.5–3.0)^{b}	1.5 (1.0–2.0)^{c}		<0.001		
Texture	3.0 (2.5–3.0)^{a}	3.0 (2.0–3.0)^{a}	2.0 (2.0–3.0)^{b}	2.0 (1.5–2.0)^{c}		<0.001		
SI[3]	3.0 (2.6–3.0)^{a}	3.0 (2.4–3.0)^{a}	2.3 (1.4–3.0)^{b}	1.5 (1.2–1.6)^{c}		<0.001		

SEM, standard error of the means. [1]Not estimated. [2]Results (medians and range) are reported as score units (1 means not acceptable; 2 means acceptable; 3 means good quality). [3]Sensory index calculated as: [(2 × odour score + 2 × colour score + 1 × texture score)/5]. [abc]Means with different superscript lowercase letter indicate significant differences between RT theses ($P < 0.05$). Refrigeration time theses (days *post-mortem*): ≤2 (2 d), 3–6 (6 d), 7–10 (10 d) and 11–14 (14 d).

significant functions, CAN1 and CAN2 (Wilks' λ = 0.001, approx. *F* value = 19.4, df1 = 96, df2 = 1833, $P < 0.001$) which explained 64.4 and 24.9% of the total variability, respectively. For the portable NIR instrument, 10 wavelengths were sorted as the most informative by the Stepwise procedure (Table 3). The CDA algorithm defined two canonical functions (CAN1 and CAN2) that showed a high discriminative power (Wilks' λ = 0.094, approx. *F* value = 9.9, df1 = 30, df2 = 241, $P < 0.001$), which accounted for 80.0 and 13.5% of the total variability, respectively. As shown in Figure 3A, for the bench-top system, the CDA model highlighted the possibility of satisfactory separation of the 0.95 confidence ellipses, even though there was a partial overlap between the two shorter shelf life theses. This discriminative capacity was confirmed by the significant D^2-Mahalanobis values, which ranged from 17.4 to 121.5 ($P < 0.001$). For the portable instrument (Figure 3B), there was a moderate spread of the 0.95 confidence ellipses across the two main canonical functions, with a partial overlap between the three shorter RT theses (2 d, 6 d, 10 d) as confirmed by the lower D^2-Mahalanobis values, which ranged from 2.8 to 20.6 ($P < 0.001$).

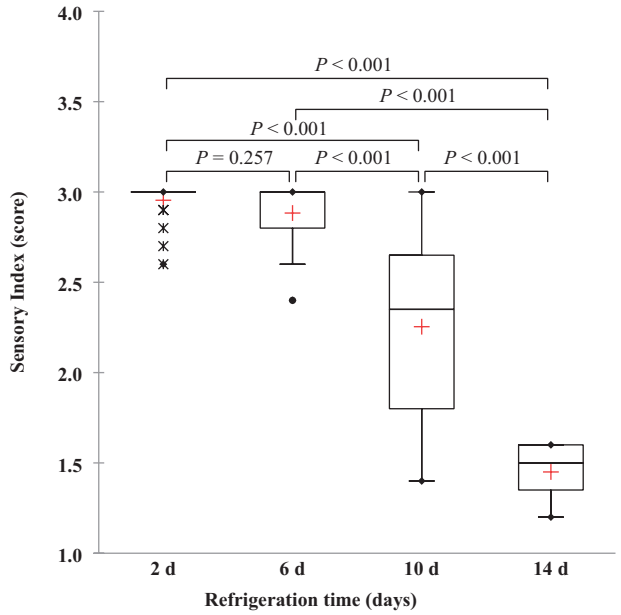

Figure 2. Box–whisker plot of sensory index (SI) across refrigeration time (RT) theses. The box plot represents the following descriptive statistics: median (bar in box), mean (+, red cross), 25–75% quartile (bottom and top end of the box), minimum and maximum values (whiskers) except for outliers (circles, distance to box 1.5–3.0 times interquartile range) and extreme values (* asterisks, distance to box > 3 times interquartile range). The significance (*P*-values on the top) of the pairwise multiple comparisons among the four RT theses was determined by Kruskal–Wallis non-parametric test (Steel–Dwass–Critchlow–Fligner correction). Refrigeration time theses (days *post-mortem*): ≤2 (2 d), 3–6 (6 d), 7–10 (10 d) and 11–14 (14 d).

The discriminating ability of the instruments was further investigated by means of a leave-one-out cross-validation to assess if the Stepwise-CDA classification functions allowed correct assignment of each chicken breast sample to its actual RT thesis (Table 4). The related confusion matrix shows how the bench-top is able to accurately distinguish all the theses (MCC > 0.94). Moreover, the bench-top instrument proves to be extremely reliable for discriminating fresh samples (2 d) compared to spoiled ones (10 d). There was a negligible misclassification of fresh samples, assigned to a class of lower freshness (6 d), which seemed to limit the monitoring effectiveness during the early stage of storage (fresh vs acceptable). However, there was no misclassification of samples with a shelf life longer than six days, thus ensuring meat safety. The portable instrument showed the lowest discriminatory capacity (MCC > 0.45) because it accurately recognised only the rotten class (MCC = 1.00), but showed a high level of misclassification between acceptable and spoiled samples (Table 4). However, it is noticeable that the discrimination performance seemed to be more reliable for fresh samples than for low-quality breast samples, and only one sample was misclassified as spoiled (MCC of 0.75). The CDA algorithm also confirmed the better discriminative capacity of bench-top with respect to portable instrument, which was previously explained in the PLS-DA paragraph.

NIR spectra, VIP and SPS and shelf life interpretation

Analysis of the discriminative models indicated a strong progressive separation during the shelf life of the refrigerated chicken breasts.

Table 2. Classification performance of PLS-DA (venetian blind cross-validation criterion) for the four chicken breast refrigeration time (RT) theses based on bench-top and portable NIR instruments

Predicted	Bench-top				Predicted	Portable			
	Actual					Actual			
	2 d	6 d	10 d	14 d		2 d	6 d	10 d	14 d
2 d	**19**	3	0	0	2 d	**16**	5	4	1
6 d	3	**19**	1	0	6 d	6	**13**	6	1
10 d	1	1	**22**	1	10 d	2	6	**11**	1
14 d	1	1	1	**23**	14 d	0	0	3	**21**
Total	24	24	24	24	**Total**	24	24	24	24
Sensitivity	0.79	0.79	0.92	0.96		0.67	0.54	0.43	0.88
Specificity	0.96	0.94	0.96	0.96		0.86	0.82	0.88	0.96
Accuracy	0.92	0.91	0.95	0.96		0.81	0.75	0.77	0.94
Precision	0.86	0.83	0.88	0.88		0.62	0.50	0.55	0.88
MCC	0.77	0.75	0.86	0.76		0.51	0.35	0.36	0.58

Refrigeration time theses (days *post-mortem*): ≤ 2 (2 d), 3–6 (6 d), 7–10 (10 d) and 11–14 (14 d). Bold values represent samples classified correctly. PLS-DA, partial least squares discriminant analysis; NIR, near-infrared; MCC, Matthews correlation coefficient.

Table 3. CDA statistics according to preliminary Stepwise and Boruta feature selection for discrimination of chicken breast refrigeration time by bench-top and portable NIR instruments

CDA statistics	Bench-top		Portable	
	Stepwise	Boruta	Stepwise	Boruta
Selected variables	32[a]	29[b]	10[c]	9[d]
Wilks' λ	0.001	0.010	0.094	0.169
CAN1 (%)	64.4	54.9	80.0	74.0
CAN2 (%)	24.9	26.2	13.5	15.7
D^2-Mahalanobis				
2 d vs 6 d	40.0	17.4	4.1	2.8
2 d vs 10 d	65.3	24.2	4.8	3.6
2 d vs 14 d	121.5	37.6	20.6	14.0

Wilks' λ and D^2-Mahalanobis always had a highly significant value ($P < 0.001$). CDA predictive scores (selected wavelengths, λ_{nm}):

[a]λ_{1174}, λ_{1206}, λ_{1302}, λ_{1406}, λ_{1430}, λ_{1454}, λ_{1470}, λ_{1478}, λ_{1518}, λ_{1870}, λ_{1886}, λ_{1894}, λ_{1902}, λ_{1974}, λ_{1982}, λ_{2006}, λ_{2086}, λ_{2110}, λ_{2206}, λ_{2222}, λ_{2230}, λ_{2334}, λ_{2358}, λ_{2366}, λ_{2374}, λ_{2390}, λ_{2398}, λ_{2422}, λ_{2430}, λ_{2438}, λ_{2462}, λ_{2490};

[b]λ_{1104}, λ_{1520}, λ_{1528}, λ_{1544}, λ_{1880}, λ_{1888}, λ_{1904}, λ_{1928}, λ_{1936}, λ_{1952}, λ_{2032}, λ_{2048}, λ_{2056}, λ_{2064}, λ_{2072}, λ_{2080}, λ_{2088}, λ_{2104}, λ_{2304}, λ_{2328}, λ_{2424}, λ_{2432}, λ_{2440}, λ_{2448}, λ_{2456}, λ_{2464}, λ_{2480}, λ_{2488}, λ_{2490};

[c]λ_{928}, λ_{1014}, λ_{1122}, λ_{1168}, λ_{1218}, λ_{1488}, λ_{1534}, λ_{1542}, λ_{1562}, λ_{1584};

[d]λ_{928}, λ_{1116}, λ_{1356}, λ_{1366}, λ_{1082}, λ_{1094}, λ_{1098}, λ_{1122}, λ_{1530}.

Refrigeration time theses (days post mortem): ≤2 (2 d), 3–6 (6 d), 7–10 (10 d) and 11–14 (14 d). CDA, canonical discriminant analysis; NIR, near-infrared; CAN1 and CAN2, two canonical functions.

Indeed, the overall results highlighted a moderate capacity of NIR spectroscopy to differentiate refrigerated poultry meat of the two shorter RT theses, probably due to mild biochemical and spoilage changes (Alexandrakis *et al.*, 2012). The findings for the chemometric models suggest that the effectiveness of NIR spectroscopy to correctly assess poultry meat shelf life seems to have a 6-day threshold for the bench-top tool, a cut-off that was delayed to around eight days for the portable one. These evidences are also supported by the results of SI that detected around 25% of spoiled samples within 10 d thesis (Figure 2). These performances are related to a simultaneous increase of many dominant NIR bands arising from the overall vibrations, overtones and combination bonds in functional groups such as –H, N–H, C–H and S–H (Liu *et al.*, 2001; Alamprese *et al.*, 2013; Barbin *et al.*, 2015). In this section, a deep biochemical interpretation of NIR wavelengths is carried out, evaluating the raw spectra, VIP indices and Stepwise-CDA predictive scores (SPS) patterns.

The raw spectra for experimental theses are reported in Figure 4, partitioned by the two NIR instruments. The distribution and magnitude of the main absorption bands observed in the present study agreed with those reported by Barbin *et al.* (2015) and Alexandrakis *et al.* (2012) referring to a wide region including the 900–2500 nm range of the applied instruments. Four high absorption bands are noticeable around 980, 1190, 1460 and 1930 nm, which are attributed to water absorption, protein changes and the effect of bacterial spoilage metabolites corresponding to O–H, C–H, NH_2 and $CONH_2$ stretching and bending, first, second and third overtones, and combination bands (Liu *et al.*, 2001; Alexandrakis *et al.*, 2012; Barbin *et al.*, 2015). The main difference between the two instruments was that the portable tool recorded high absorption values for the prolonged shelf life theses, whereas the bench-top instrument showed the opposite trend (Figure 4). The rotten thesis is the storage phase

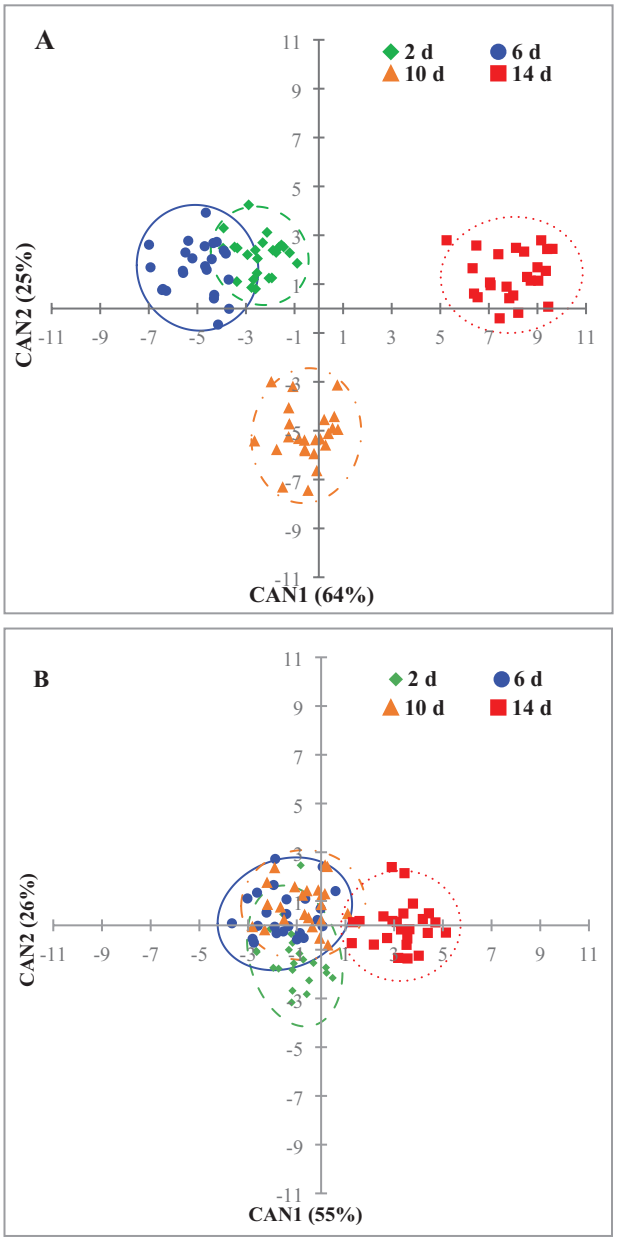

Figure 3. Stepwise-CDA scatterplots of the four chicken breast refrigeration time (RT) theses according to bench-top (**A**) and portable (**B**) NIR instruments; the 0.95 confidence ellipses are drawn around each centroid of groupings. RT theses (days *post-mortem*): ≤2 (2 d): green dotted line and diamonds; 3–6 (6 d): blue solid line and dots; 7–10 (10 d): orange dotted-pointed line and triangles; 11–14 (14 d): red pointed line and squares. CAN1 and CAN2, two canonical functions; CDA, canonical discriminant analysis; NIR, near-infrared.

with the highest muscle denaturation and intense proteolysis that increase the movement of water from intracellular into extracellular spaces (Bowker *et al.*, 2014). This means that a prolonged shelf life reduces the water holding capacity (WHC), increasing drip losses and NIR spectral absorbance, as in the case of portable tool, since free water is retained on the breast surface. The significant increase of L* values observed in the rotten theses was related to the release of exudates on breasts surface (Table 1). With regard to the bench-top instrument, mincing the samples promotes a partial loss of this water, with a probable subsequent reduction in absorption.

Table 4. Classification performance of Stepwise-CDA (leave-one-out cross-validation criterion) for the four chicken breast refrigeration time (RT) theses based on bench-top and portable NIR instruments

Predicted	Bench-top				**Predicted**	Portable			
	Actual					Actual			
	2 d	6 d	10 d	14 d		2 d	6 d	10 d	14 d
2 d	**22**	0	0	0	2 d	**20**	4	2	0
6 d	2	**24**	0	0	6 d	3	**13**	7	0
10 d	0	0	**24**	0	10 d	1	7	**15**	0
14 d	0	0	0	**24**	14 d	0	0	0	**24**
Total	24	24	24	24	**Total**	24	24	24	24
Sensitivity	0.92	1.00	1.00	1.00		0.83	0.54	0.61	1.00
Specificity	1.00	0.97	1.00	1.00		0.92	0.83	0.89	1.00
Accuracy	0.98	0.98	1.00	1.00		0.90	0.75	0.82	1.00
Precision	1.00	0.92	1.00	1.00		0.77	0.57	0.64	1.00
MCC	0.94	0.95	1.00	1.00		0.75	0.45	0.54	1.00

Refrigeration time theses (days post-mortem): ≤ 2(2 d), 3–6 (6 d), 7–10 (10 d) and 11–14 (14 d). Bold values represent samples classified correctly. CDA, canonical discriminant analysis; MCC, Matthews correlation coefficient.

An in-depth scrutiny of absorbance related to different chemical compounds could also help better understand meat behaviour during refrigeration. The VIP and SPS procedures captured a multitude of spectral information (Figure 5). The bench-top chilling preservation profile highlighted many significant VIP indices (>1.0), which represent the most relevant spectral features in the ranges 1100–1160, 1300–1350, 1380–1400 and 1850–1900 nm, and other additional features in the ranges 2050–2350 and over 2400 nm. Instead, the portable system refrigerated storage VIP pattern resulted in just three informative (>1.0) wavelengths belonging to the following spectral ranges: 1200–1250, 1350–1450 and over 1500 nm. With regard to SPS, these selected wavelengths belonged to four main spectral regions corresponding to 1200–1250, 1300–1500, 1900–2000 and over 2100 nm for bench-top system, and just two regions, 900–1200 and 1500–1580 nm, for portable one.

In general, the absorptions observed in the NIR region are overtones or combinations of the fundamental stretching bands which are usually due to C–H, N–H or O–H stretching mode (Cen and He, 2007). As confirmed by the physicochemical and sensorial analyses carried out as preliminary step (Table 1), *post-mortem* processes cause several biochemical changes including pH modification (i.e. early muscle acidification), alteration of cellular compartmentalisation, release of free catalytic iron, and myofibrillar contraction (Mir *et al.*, 2017). During meat storage, a shift in absorbance bands may be induced by changes that occur in proteins, due to the action of oxidising enzymes promoting the formation of protein carbonyls, and in lipids, due to the evolution of oxidative reactions, resulting in the formation and release of secondary products including lipid alcohols, ketones, epoxides, aldehydes and hydrocarbons (Estévez, 2011) that affected odour acceptability (Table 1). Overall, physicochemical modifications of meat structure induce a decrease in WHC, a change in surface colour and the development of microbial spoilage (Mir *et al.*, 2017). We have attempted to explain the significance of VIP and SPS in terms of the relationship between these muscle chemical changes and NIR spectral patterns, for both bench-top and portable, during 14 days of chicken breast storage.

Compared to the portable one, the bench-top instrument provides a wide range of spectral information suitable for the in-depth interpretation of biochemical and spoilage phenomena causing meat deterioration (Figure 5A). Thus, we focus the following discussion on the bench-top tool, even though the few VIPs for the portable one, found around 1190, 1370, 1400, 1440 and 1600 nm, are involved in the same biochemical processes described below. The 1100–1400 nm region is mainly characterised by the second overtones of C–H stretching and vibration modes associated with carbonyl formation (Alamprese *et al.*, 2016), which is an irreversible and non-enzymatic process involving the formation of carbonyl moieties and further aldehydes and ketones by the oxidation of many amino acids (Estévez, 2011). Probably, these chemical pathways related to carbonylation are recognised by NIR spectroscopy because they affect the vibration of functional groups. Several VIPs were observed at wavelengths related to water interactions through hydrogen bonds and other meat components (Nolasco Perez *et al.*, 2018). A few broad and high VIP scores are noticeable around the region of the first overtone of water, especially the wavelengths around 1384–1388 nm that could be assigned to H_2O–OH-bonded water molecules, while around 1410 nm the VIPs are mainly related to free water molecular species (Tsenkova *et al.*, 2015). Indeed, the 1400–1600 nm region basically includes the first overtones of the O–H/N–H stretching modes of self-associated and water-bonded OH/NH groups of N-compounds in meat (Liu *et al.*, 2001). Once again, changes in this spectral region could be linked to protein denaturation, proteolysis and WHC reduction. Thus, the physical relationship between water molecular species and protein and lipid C–H/N–H seem to be the major contributors to sample shelf life differentiation. In this study, additional weak sharp spectral markers were found at 1700 and 1732 nm, corresponding to the first overtones of C–H stretching modes, which might be linked to a change in lipid deterioration (Ding *et al.*, 1999; Peng and Wang, 2015). The NIR spectra of chicken meat showed a prominent VIP in the absorbance region 1850–1910 nm, specific to O–H functional groups, H_2O overtones and vibration of O–H bonds (1920 nm) (Alamprese *et al.*, 2016; Ghidini *et al.*, 2019). Specific carbonyl and N–H asymmetric stretching has been reported in this region, probably due to amides and amines, major N-catabolites arising from the late proteolytic process (Alamprese *et al.*, 2016). A strong relationship between informative bands and both amides and amines has already been reported by the authors in Alexandrakis *et al.* (2012), as a consequence of prolonged storage associated with ammonia and volatile amines from free amino acids and peptides related to autolytic and microbial enzyme activity (Alexandrakis *et al.*, 2012). The second overtone of carbonyl groups related to peptides, aldehydes and ketones has been already selected at 1900–1960 nm, even though

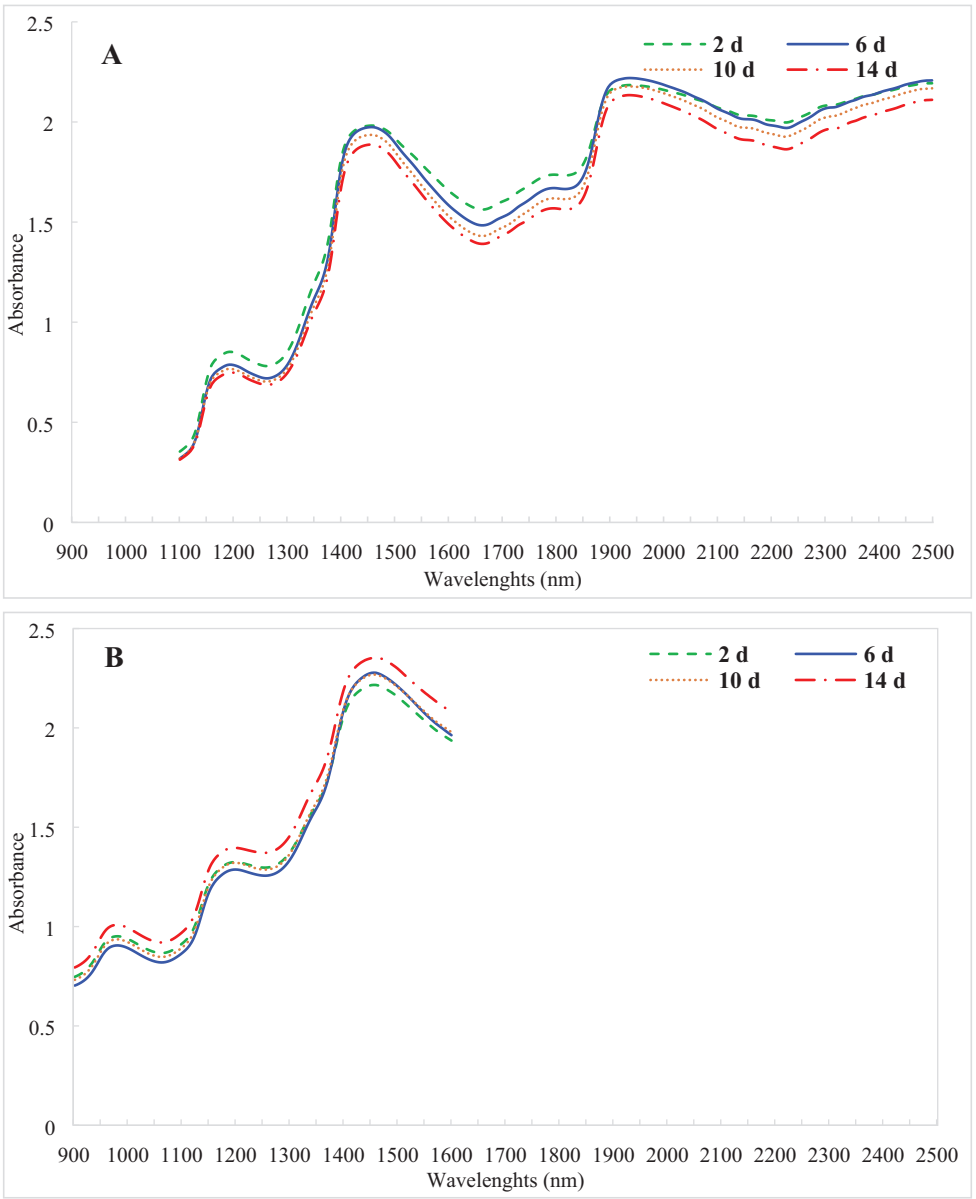

Figure 4. Average spectra of the four refrigeration time (RT) theses related to bench-top (**A**) and portable (**B**) NIR instruments. Refrigeration time theses (days *post-mortem*): ≤2 (2 d), 3–6 (6 d), 7–10 (10 d) and 11–14 (14 d). NIR, near-infrared.

these wavelengths are overlap with the water band at 1940 nm (Jha, 2010). The 2040–2350 nm region might be associated with myoglobin N–H bonds (Burns and Ciurczak, 2008) and related to C–H combination tones (2340 nm) of unsaturated fatty acids (Cozzolino *et al.*, 2002; Peng and Wang, 2015).

Interpretation of the SPS feature variables was similar to that for VIP indices previously mentioned. These were partly overlapping or closer to the VIPs previously described. However, around 1000, 1500, 2000 and 2400 nm, in particular in λ_{1014}, λ_{1488} (for portable instrument), λ_{1174}, λ_{1206}, λ_{1430}, λ_{1454}, λ_{1470}, λ_{1478}, λ_{1518}, λ_{1974}, λ_{1982}, λ_{2006}, λ_{2358}, λ_{2366}, λ_{2374}, λ_{2390} and λ_{2398} (for bench-top instrument), the SPS are distant from the VIP peaks, but identify themselves in wavelengths that express those biochemical processes already described.

The findings of this study suggested that the VIPs pattern and SPS could be useful markers of meat deterioration related to proteolysis (1100–1400 and 1850–1920 nm) and amino acids oxidation (1400–1600 nm), lipid oxidation (1700–1740 nm) and decrease in WHC (1380–1410 nm). Moreover, we advise the use of the selected spectral ranges described above, as a NIR benchmark for a rapid assessment of spoilage threshold of chicken breasts.

Conclusions

Overall results of the present experiment highlighted that NIR technology could be considered a potential safety and quality labelling tool to prevent deceptive practices related to meat freshness, both for food industry and consumer protection. The combination of NIR technology with discriminating chemometric approaches potentially allowed a reliable assessment of chicken breasts shelf life, with a refrigeration cut-off of a week. Based on a multivariate model, a selection of NIR features were suitable for the interpretation of the main physicochemical changes during poultry meat storage.

Based on actual findings, the bench-top tool seemed to be more effective for predicting chicken breast shelf life than the portable

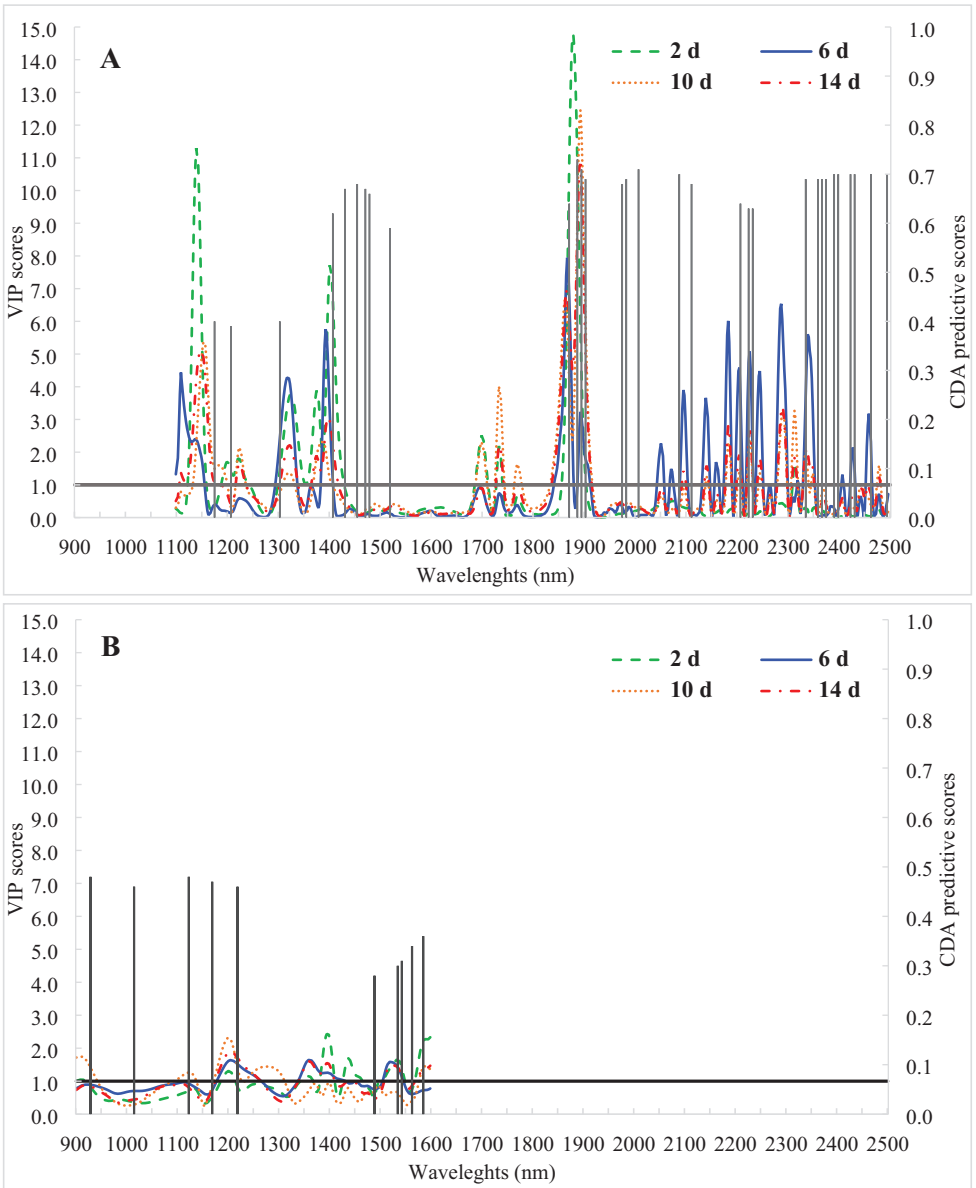

Figure 5. VIP index scores obtained by PLS-DA algorithm and CDA predictive scores (SPS) sorted by the Stepwise feature selection procedure according to the four refrigeration time (RT) theses related to bench-top (**A**) and portable (**B**) NIR instruments. Refrigeration time theses (days *post-mortem*): ≤2 (**2 d**), 3–6 (**6 d**), 7–10 (**10 d**) and 11–14 (**14 d**). VIP, variable importance in projection; PLS-DA, partial least squares discriminant analysis; CDA, canonical discriminant analysis; NIR, near-infrared.

one, probably due to better optical properties and the longer spectral range. Considering an operative scenario, the challenge of portable NIR instruments could be its suitability for rapid at-line screening of poultry meat along the supply chain in a real enterprise environment. Meanwhile, the application of the bench-top NIR might be proposed as spectroscopy gold standard for evaluating the shelf life of fresh cuts. Perhaps it could be useful for minced meat quality control and meat preparation at the slaughterhouse and in cutting plants. Further experimental trials are needed to improve the accuracy and reliability of the portable spectrometer in detecting biochemical meat changes.

Author Contributions

Ilaria Lanza: Data curation, interpreted the results and wrote the manuscript. Daniele Conficoni, Marco Cullere, Angela Trocino, Gerolamo Xiccato: Writing the manuscript. Stefania Balzan, Luca Fasolato, Enrico Novelli, Severino Segato: Conceptualization, planned the experiment, carried out the experiments, interpreted the results and wrote the manuscript. Lorenzo Serva, Barbara Contiero: Data Curation, statistical analyses, interpreted the results. Enrico Novelli, Severino Segato: Funding acquisition.

Funding

This works was supported by FONDAZIONE CARIVERONA (projects Tre Poli 4 and 6, call 2012 and 2016); University of Padova (2019 SID assignment), Italy.

Conflict of Interest

The authors declare no conflict of interest.

References

Akarachantachote, N., Chadcham, S., Saithanu, K. (2014). Cutoff threshold of variable importance in projection for variable selection. *International Journal of Pure and Applied Mathematics*, 94: 307–322.

Alamprese, C., Casale, M., Sinelli, N., *et al.* (2013). Detection of minced beef adulteration with turkey meat by UV-vis, NIR and MIR spectroscopy. *LWT - Food Science and Technology*, 53: 225–232.

Alamprese, C., Amigo, J. M., Casiraghi, E., *et al.* (2016). Identification and quantification of turkey meat adulteration in fresh, frozen-thawed and cooked minced beef by FT-NIR spectroscopy and chemometrics. *Meat Science*, 121: 175–181.

Alexandrakis, D., Downey, G., Scannell, A. G. M. (2012). Rapid non-destructive detection of spoilage of intact chicken breast muscle using near-infrared and Fourier transform mid-infrared spectroscopy and multivariate statistics. *Food and Bioprocess Technology*, 5: 338–347.

Atanassova, S., Stoyanchev, T., Yorgov, D., *et al.* (2018). Differentiation of fresh and frozen-thawed poultry breast meat by near infrared spectroscopy. *Bulgarian Journal of Agricultural Science*, 24: 162–168.

Barbin, D. F., Kaminishikawahara, C. M., Soares, A. L., *et al.* (2015). Prediction of chicken quality attributes by near infrared spectroscopy. *Food Chemistry*, 168: 554–560.

Bisutti, V., Merlanti, R., Serva, L., *et al.* (2019). Multivariate and machine learning approaches for honey botanical origin authentication using near infrared spectroscopy. *Journal of Near Infrared Spectroscopy*, 27: 65–74.

Bowker, B., Hawkins, S., Zhuang, H. (2014). Measurement of water-holding capacity in raw and freeze-dried broiler breast meat with visible and near-infrared spectroscopy. *Poultry Science*, 93(7): 1834–1841.

Bruckner, S., Albrecht, A., Petersen, B., *et al.* (2012). Characterization and comparison of spoilage processes in fresh pork and poultry. *Journal of Food Quality*, 35: 372–382.

Burns, D. A., Ciurczak, E. W. (2007). Handbook of near-infrared analysis. Taylor & Francis Group, Boca Raton, FL, pp. 521–527.

Cen, H. Y., He, Y. (2007). Theory and application of near infrared reflectance spectroscopy in determination of food quality. *Trends in Food Science and Technology*, 18: 72–83.

Cozzolino, D., De Mattos, D., Vaz Martins, D. (2002). Visible/near infrared reflectance spectroscopy for predicting composition and tracing system of production of beef muscle. *Animal Science*, 74: 477–484.

Crocombe, R. A. (2018). Portable spectroscopy. *Applied Spectroscopy*, 72(12): 1701–1751.

Ding, H. B., Xu, R. J., Chan, D. K. O. (1999). Identification of broiler chicken meat using a visible / near-infrared spectroscopic technique. *Journal of the Science of Food and Agriculture*, 79: 1382–1388.

Estévez, M. (2011). Protein carbonyls in meat systems: a review. *Meat Science*, 89: 259–279.

Falkovskaya, A., Herrero-Langreo, A., Gowen, A. (2019). Comparison of Vis-Nir (400–1,000 Nm) and Nir (978–1,678 Nm) hyperspectral imaging for discrimination between fresh and previously frozen poultry. 2019 10th Workshop on Hyperspectral Imaging and Signal Processing: Evolution in Remote Sensing (WHISPERS). 24-26 September 2019, IEEE, Amsterdam, Netherlands, pp. 1–5.

FAO (The Food and Agriculture Organization). (2020a). FAOSTAT [Online]. http://www.fao.org/faostat/en/#home. Accessed on June 10, 2020.

FAO (The Food and Agriculture Organization). (2020b). Gateway to Poultry Production and Products [Online]. http://www.fao.org/poultry-production-products/en/. Access on June 10, 2020.

Fernández-Pan, I., Carrión-Granda, X., Maté, J. I. (2014). Antimicrobial efficiency of edible coatings on the preservation of chicken breast fillets. *Food Control*, 36: 69–75.

Ghidini, S., Varrà, M. O., Zanardi, E. (2019). Approaching authenticity issues in fish and seafood products by qualitative spectroscopy and chemometrics. *Molecules*, 24: 1812.

Gram, L., Ravn, L., Rasch, M., *et al.* (2002). Food spoilage–interactions between food spoilage bacteria. *International Journal of Food Microbiology,* 78(1–2): 79–97.

Gratta, F., Fasolato, L., Birolo, M., *et al.* (2019). Effect of breast myopathies on quality and microbial shelf life of broiler meat. *Poultry Science*, 98(6): 2641–2651.

Jha, S. N. (2010). Near infrared spectroscopy. In: Nondestructive evaluation of food quality: theory and practice. Springer Science & Business Media, Berlin, Germany.

Katiyo, W., de Kock, H. L., Coorey, R., *et al.* (2020). Sensory implications of chicken meat spoilage in relation to microbial and physicochemical characteristics during refrigerated storage. *LWT - Food Science and Technology*, 128: 109468.

Kursa, M. B., Rudnicki, W. R. (2010). Feature selection with the boruta package. *Journal of Statistical Software*, 36: 1–13.

Leardi, R. (2000). Application of genetic algorithm-PLS for feature selection in spectral data sets. *Journal of Chemometrics*, 14: 643–655.

Liu, Y., Chen, Y. R., Ozaki, Y. R. (2001). Two-dimensional visible / near-infrared correlation spectroscopy study of thermal treatment of chicken meats. *Meat Science*, 54: 1458–1470.

Melro, E., Antunes, F., Cruz, I. *et al.* (2020). Morphological, textural and physico-chemical characterization of processed meat products during their shelf life. *Food Structure*, 26: 100164.

Mendez, J., Mendoza, L., Cruz-Tirado, J. P., *et al.* (2019). Trends in application of NIR and hyperspectral imaging for food authentication. *Scientia Agropecuaria*, 10: 143–161.

Mir, N. A., Rafiq, A., Kumar, F., *et al.* (2017). Determinants of broiler chicken meat quality and factors affecting them: a review. *Journal of Food Science and Technology*, 54(10): 2997–3009.

Morsy, N., Sun, D. W. (2013). Robust linear and non-linear models of NIR spectroscopy for detection and quantification of adulterants in fresh and frozen-thawed minced beef. *Meat Science*, 93(2): 292–302.

Nolasco Perez, I. M., Badaró, A. T., Barbon, S. Jr, *et al.* (2018). Classification of chicken parts using a portable near-infrared (NIR) spectrophotometer and machine learning. *Applied Spectroscopy*, 72(12): 1774–1780.

Ottavian, M., Franceschin, E., Signorin, E., *et al.* (2015). Application of near infrared reflectance spectroscopy (NIRS) on faecal samples from lactating dairy cows to assess two levels of concentrate supplementation during summer grazing in alpine pastures. *Animal Feed Science and Technology*, 202: 100–105.

Peng, Y. K., Wang, W. X. (2015). Application of near-infrared spectroscopy for assessing meat quality and safety. In: Infrared Spectroscopy - Anharmonicity of Biomolecules, Crosslinking of Biopolymers, Food Quality and Medical Applications. InTech, London, UK.

Raab, V., Bruckner, S., Beierle, E., *et al.* (2008). Generic model for the prediction of remaining shelf life in support of cold chain management in pork and poultry supply chains. *Journal on Chain and Network Science*, 8: 59–73.

Rubingh, C. M., Bijlsma, S., Derks, E. P., *et al.* (2006). Assessing the performance of statistical validation tools for megavariate metabolomics data. *Metabolomics: Official Journal of the Metabolomic Society*, 2(2): 53–61.

Segato, S., Merlanti, R., Bisutti, V., *et al.* (2019). Multivariate and machine learning models to assess the heat effects on honey physicochemical, colour and NIR data. *European Food Research and Technology*, 245: 2269–2278.

Sivarajan, M., Lalithapriya, U., Mariajenita, P., *et al.* (2017). Synergistic effect of spice extracts and modified atmospheric packaging towards non-thermal preservation of chicken meat under refrigerated storage. *Poultry Science*, 96(8): 2839–2844.

Sujiwo, J., Kim, D., Jang, A. (2018). Relation among quality traits of chicken breast meat during cold storage: correlations between freshness traits and torrymeter values. *Poultry Science*, 97(8): 2887–2894.

Teixeira dos Santos, C. A., Lopo, M., Páscoa, R. N., *et al.* (2013). A review on the applications of portable near-infrared spectrometers in the agro-food industry. *Applied Spectroscopy*, 67(11): 1215–1233.

Tsenkova, R., Kovacs, Z., Kubota, Y. (2015). Aquaphotomics: near infrared spectroscopy and water states in biological systems. *Sub-Cellular Biochemistry*, 71: 189–211.

Xu, X., Xie, L. J., Ying, Y. B. (2019). Factors influencing near infrared spectroscopy analysis of agro-products: a review. *Frontiers of Agricultural Science and Engineering*, 6: 105–115.

Zareef, M., Chen, Q., Hassan, M. M., *et al.* (2020). An overview on the applications of typical non-linear algorithms coupled with NIR spectroscopy in food analysis. *Food Engineering Reviews*, 12: 173–190.

Zhao, G., Maclean, A. L. (2000). A comparison of canonical discriminant analysis and principal component analysis for spectral transformation. *Photogrammetric Engineering and Remote Sensing*, 66: 841–847.